Biomimetic model of a sponge-spicular optical fiber—mechanical properties and structure

M. Sarikaya,[a] H. Fong, N. Sunderland, B.D. Flinn, and G. Mayer
Materials Science and Engineering, University of Washington, Seattle, Washington 98195

A. Mescher
Mechanical Engineering, University of Washington, Seattle, Washington 98195

E. Gaino
Instituto di Zoologia dell'Universita di Perugia, Perugia, Italy

(Received 10 October 2000; accepted 26 February 2001)

Nanomechanical properties, nanohardness and elastic modulus, of an Antarctic sponge *Rosella racovitzea* were determined by using a vertical indentation system attached to an atomic force microscope. The Rosella spicules, known to have optical waveguide properties, are 10–20 cm long with a circular cross section of diameter 200–600 μm. The spicules are composed of 2–10-μm-thick layers of siliceous material that has no detectable crystallinity. Measurements through the thickness of the spicules indicated uniform properties regardless of layering. Both the elastic modulus and nanohardness values of the spicules are about half of that of either fused silica or commercial glass optical fibers. The fracture strength and fracture energy of the spicules, determined by 3-point bend tests, are several times those of silica rods of similar diameter. These sponge spicules are highly flexible and tough possibly because of their layered structure and hydrated nature of the silica. The spicules offer bioinspired lessons for potential biomimetic design of optical fibers with long-term durability that could potentially be fabricated at room temperature in aqueous solutions.

I. INTRODUCTION

The transmission of light through glass fiber typically brings to mind applications in the flourishing telecommunications industry.[1,2] In this article, however, we report on the unique properties of an optical fiber that occurs naturally in a sponge species Rosella.[3] Our childhood experiences, such as broken windows, glass cups and bottles, remind us that glass is fragile. In fact, the use of glass fiber in technological applications is only possible with polymeric coating that significantly improves the mechanical durability of fibers by sealing the surface cracks and by providing a barrier to water and other contaminants.[4] As we show in this article, even more impressive are mechanical properties of a sponge spicule, a hydrated siliceous glass, used as a waveguide by a sponge species, Rosella, that produces it under seemingly rudimentary synthesis conditions from seawater.

Many multicellular and single-celled organisms produce hard tissues, such as bones, teeth, shells, skeletal units, particles, surface layers, spicules, and spines.[5,6] These biological materials are composites of minerals, perhaps 60 different kinds, and organic macromolecules, a combination of proteins, polysaccharides, and lipids. Normally, hard tissues are mechanical devices (skeletal units, protective armor, and anchoring devices), but they also have other physical functions, such as magnetic, optical, and piezoelectric. The biological hard tissues have extraordinary physical properties, not achieved in synthetic composites with similar phase compositions. This is attributed to their highly ordered, often, hierarchical structures that are controlled from the nanometer to the micrometer and higher-dimensional scales by the organic components, mostly by proteins. Biological materials are synthesized by the organisms at mild conditions (in aqueous solutions at pH approximately 7.0, room temperature, and pressure) and yet have desirable engineering properties. These systems may offer bioinspired lessons for design and processing of a new class of advanced materials based on biomimetic lessons from nature.

In this article, we discuss the structural and mechanical properties of a functional hard tissue, a sponge spicule that has unique optical characteristics. Depending on the sponge species, spicules may be used as skeletal components providing a support structure for the animal, deterrents against predators; or as anchors allowing deep-sea dwelling species to hold onto soft sedimentary ocean

[a]Address all correspondence to this author.
e-mail: sarikaya@u.washington.edu

https://doi.org/10.1557/JMR.2001.0198

floors.[7] Spicule dimensions range in diameter from only a few micrometers to several millimeters and in length from several tens of micrometers to tens of millimeters and even longer. The demosponge species we used in this work is *Rosella racovitzea* (Rosella).[8] Its spicules are $\geqslant$10 cm with cross-shaped apexes that may serve to collect light. The species lives 100–200 m underwater near Antarctica. The presence of a filamentous green algae, a chlorophyte adapted to dim light conditions, suggests that light may reach the inside of the sponge body via these siliceous spicules acting as optical wave-guides.[9] In this scenario, sponge/algae form a symbiotic system in which the spicules are optical lenses and fibers, gathering and transferring the dim light present at these depths to the algae (*Ostreobium constrictum*), which transfers the nutrients to the sponge.[10]

In a recent publication, we measured optical properties of the Rosella spicule and compared them with synthetic optical fibers.[11] We found that the index of refraction ($n = 1.49$), constant throughout the thickness, is similar to that of commercial silica fiber. In addition, the numerical aperture of the spicule is 0.44, and the angle of acceptance is 52°. These optical properties suggested to us that the Rosella spicules have characteristics comparable with those of commercial glass optical fibers. To assess durability and mechanical integrity, we then set out to determine the mechanical properties of sponge spicules and compared them with those of synthetic glass optical fibers. At the same time, we studied the sponge spicules in more detail to evaluate their microstructure and to assess whether the spicule's structure is layered or uniform throughout its thickness. Layering would indicate that the spicule could be a graded-index optical fiber,[12,13] each layer having a different index of refraction. In determining the optical properties of Rosella spicules, we had already found that the index of refraction does not change throughout the thickness, suggesting, originally, that the spicule is a solid cylindrical rod. Although the refractive index is constant throughout the spicule thickness, the spicule actually is made of silica layers with varying layer thickness, as we describe in this article. Furthermore, nanomechanical tests, conducted by using a vertical indenter attached to an atomic force microscope, indicate a constant hardness and elastic modulus values, i.e., mechanical properties in unison with optical characteristics.

To assess bulk mechanical behavior of the spicules, we also conducted 3-point bend tests. The results of these tests indicated that fracture strength, strain-to-failure, and fracture energy are several times greater than for silica glass rods with similar diameter. In addition to providing bulk mechanical properties, the bulk tests also revealed that, under bending stress, the sponge spicule undergoes "soft-failure," unlike glass rods that fail catastrophically and at significantly lower stresses. The bulk mechanical properties and soft failure of these spicules could partially be explained on the basis of their layered structure revealed in this work. Based on nano- and microstructural characteristics and mechanical properties obtained, the results in this article offer possible design guidelines for potential novel, damage-tolerant optical fibers via biomimetics.

II. EXPERIMENTAL PROCEDURES

We used the pentactinal spicules from *Rosella racovitzea* Topsent 1901 (*Porifera: Hexactinellida*),[10] sampled at 120-m depth in Terra Nova Bay (Ross Sea, Antarctica) during the PNRA XI Italian Antarctic Expedition (1994–95)[3] to test the mechanical properties and study the microstructure. The sponge Rosella is 100 cm tall and has a 30–50-cm diameter with a cylindrical geometry [Fig. 1(a)].[3,8] The spicules are located on the outside of the body and extend outward between 10 and 20 cm in length. The diameters of the spicules are nonuniform, ranging from 200 to 600 μm. The apex of each spicule has a cross-shaped structure [Figs. 1(b) and 1(c)] that is likely to be used for collecting light from all directions, a possible optical lens. Although the structure of the apex is reported in this article, the optical properties and possible formation mechanism will be discussed elsewhere.

We performed the mechanical property measurements by using the spicules with the apex removed. The spicules were kept in air, and they had surface cracks, probably induced during handling. Although these surface cracks adversely affected the fracture characteristics, the spicules still have extraordinary mechanical properties compared with synthetic silica rods. Nanoindentation with the Atomic Force Microscope (AFM) requires cross-sectional samples with fairly flat surfaces.[14,15] Polishing can produce samples with several nanometer root-mean-square (rms) roughness. Because of the small diameter of the spicules, however, they were difficult to hold during polishing. Therefore, individual fibers were embedded in an epoxy after sectioning with a razor blade to a length slightly greater than the height of the mounting cup, ensuring that they were vertical to the polishing surface. The surface was sanded down to 1200 grit, starting out with a 150 SiC paper. Final polishing was performed by using a 0.05-μm particle size alumina slurry with an autopolisher. The surface was examined both by optical light microscopy [Fig. 2(d)] and AFM (Fig. 3) to ensure a smooth cross section throughout. The polishing treatment produced a surface with an rms of 3.0 ± 1.0 nm as measured by an AFM in the contact mode. The etched samples, to observe layering in the spicules by optical microscopy, were prepared by treating the surfaces of the cross-sectional samples using a 5% aqueous nitric acid solution after the final polishing [Fig. 2(e)].

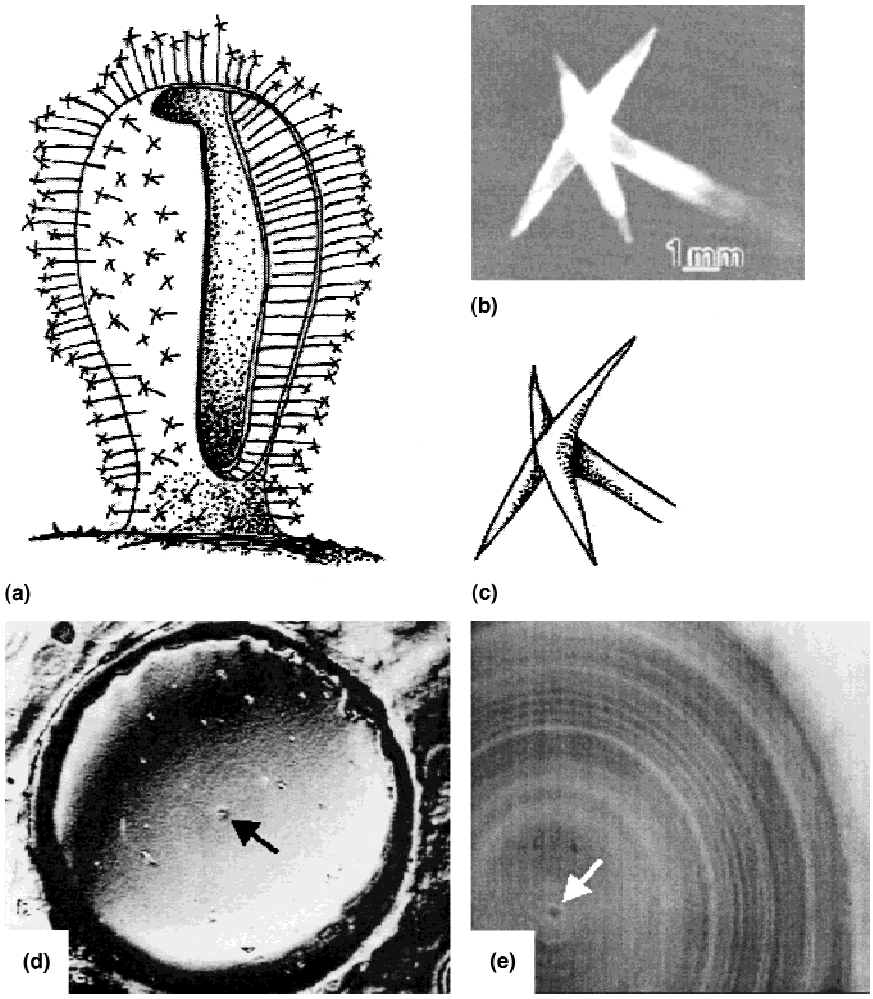

FIG. 1. (a) A schematic drawing of the sponge (adapted from Ref. 1). (b and c) A general photographic view of the stem and the apex of a Rosella spicule and a schematic drawing. Optical microscopy images of cross-sectional spicule samples after polishing (d) and polishing and etching (e). The central proteinaceous filament is shown by an arrow in (d and e).

The synthetic glass optical fibers (SMF-LS; Corning Inc., Corning, NY), coated with polymers to prevent surface cracks, had a diameter of 250 μm. Therefore, standard metallographic techniques proved futile for cutting and polishing. The fiber samples were first mounted in an epoxy. A diamond-coated wafering saw (Isomet cutter; Buehler Ltd., Lake Bluff, IL) was used to cut the cross-sectional samples. Polishing was accomplished by using a diamond paste with a particle size of 0.05 μm on a silk- or felt-covered rotating polishing disk. A final washing to clean the sample surfaces from any debris was accomplished by using methanol after which the samples were mounted on a steel puck for AFM and nanohardness measurements.

Nanoindentation was performed by using a Hysitron Triboscope (a nanomechanical testing apparatus, Hysitron Co., Minneapolis, MN) attached to a ParkAutoprobe CP scanning probe microscope (Thermal Microscopes, San Jose, CA). A Berkovich diamond tip, with the {111} surfaces forming a pyramidal tip of the diamond single crystal, was used both as an imaging system and the nanoindenter. With the nanoindentation apparatus/AFM system, surface topography imaging as well as indentation could be performed sequentially at the same position allowing the analysis of the surfaces before and after indentation tests. For indentation analysis, force (F) versus displacement (d) of the load–unload cycle was obtained [Fig. 3(a)]. Hardness (H) and elastic (Young's) modulus (E) were determined from the unloading portion of the F-d curves with a known indenter tip area function (the tip area is the interface between the tip surface and the surface of the sample indented). The tip area function was calibrated by using a fused silica sample according to the procedure described in Ref. 15. Hardness and reduced elastic modulus determined from the Hysitron system is deduced from the following relations[14,15]:

$$S = P_{\max}/A$$

https://doi.org/10.1557/JMR.2001.0198

and

$$E = S(\pi)^{1/2}/2A^{1/2} \quad ,$$

where P_{max} is the maximum applied load and S is the stiffness of the system. Area of contact, A, is calibrated as a function of the contact height, h. For this study, A was calibrated for h values up to 100 nm.

All indentations were performed in air. To prevent extensive drying, the exposure to air of spicule or optical fibers was minimized. Indentations were made across the diameter of the spicules starting from the central proteinaceous filament and extending radially outward [Figs. 3(a) and 3(b)]. In glass fibers, the indentations were made from one edge across the sample diameter to the other edge. Successive indentations were taken at least 3–4 μm apart, i.e., about 3–5 times the edge size of the indents, to prevent overlap of the elastic/plastic zone that would affect test results. The applied load varied from 500 to 2500 μN until a contact depth of 100 nm was reached in all the samples tested. We found that the optimum condition required a 2000 μN for fused silica and optical fibers and 800 μN for the spicules. This magnitude of loading produced indenter edge size about 0.7–0.8 μm. The depth achieved ensured that a large enough area was sampled, and possible effects of any surface irregularity or artifactual surface variations were eliminated. Loading and unloading procedures were conducted at a rate of 400 μN/s because it was found to be the maximum rate without inducing observable creep in the *F-d* curves. Using slower loading rates did not alter the values of hardness or elastic modulus measured.

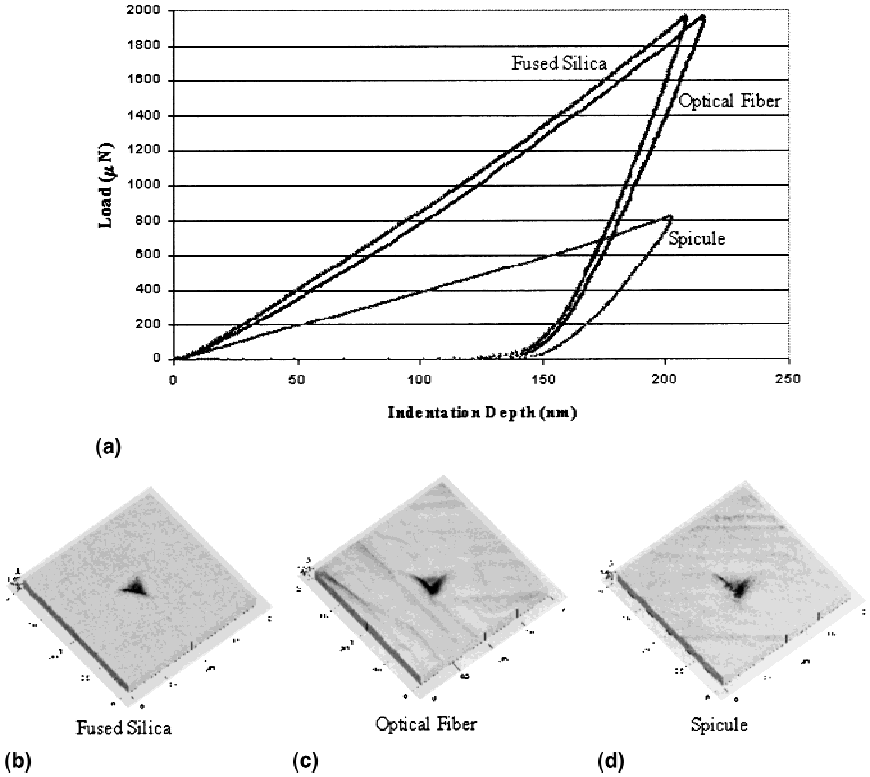

FIG. 2. (a) Force-deflection curves from nanomechanical tests of fused silica, optical fiber, and sponge spicule samples. (b), (c), and (d) are AFM images of the corresponding indentations, respectively.

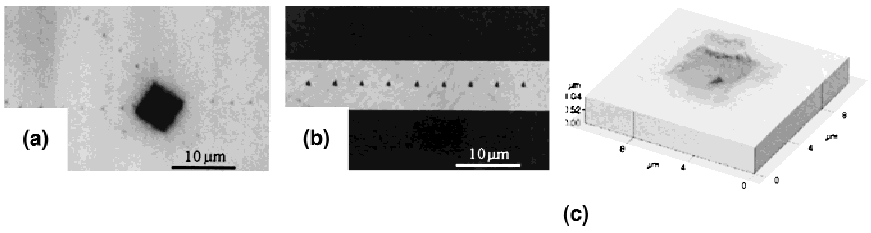

FIG. 3. (a) AFM image of the indentations across a sponge spicule sample in 2 radial directions starting from the central proteinaceous filament (square-shaped region). (b) Details of indentations through the radial direction on a spicule. (c) An AFM image of an indentation made on the central core of a spicule from a polished sample.

The indentations on each of the silica samples were validated by rescanning the indented areas with the same indenter tip (Figs. 2 and 3). This was performed to ensure that the indentations were not made on surface asperities and that they were large enough compared with the local surface roughness. An indentation made on an asperity on a polished surface would record a lower hardness (and elastic modulus) because of easy deformation of these areas. Figure 2(a) displays characteristic *F-d* curves and corresponding AFM images [Figs. 2(b)–2(d)] of the indentation from the sponge spicule, optical fiber, and fused silica, respectively, [Fig. 2(a)] recorded under optimum loading conditions. The pyramidal shape of the indent in each polished sample is clearly displayed. The clarity of the shape of the diamond indentor's impression is reflective of the reliability of the experimentally determined mechanical property values. This is important because the total stress for hardness determination was derived from the applied load over an area corresponding to a pyramidal impression.

We have also measured the flexural properties of the spicules and silica glass rods in 3-point bending (glass rods were GE-Type-214 high-purity fused silica; General Electric Co., Schenectady, NY). Samples 20–25 mm in length were tested in a 3-point-bend fixture with a 10-mm span and an articulated center loading rod at a crosshead rate of 0.5 mm/min. The diameter of the spicules ranged from 0.34 to 0.56 mm, whereas the silica rods were 1.14 mm in diameter. Tests were performed by using a computer-controlled MTS servo-hydraulic test frame (MTS Systems Co., Eden Prairie, MN). Crosshead displacement (LVDT, 10-mm full scale) and load (100 N load cell) were recorded throughout the tests.

Microstructural analysis was also conducted by using a scanning electron microscope (SEM) to reveal the details of the structure at dimensions of a micrometer and above. Samples for SEM were either fractured at room temperature or first plunged into liquid nitrogen and then fractured in air. This ensured that the fracture took place by a critically sized crack following the weakest path. The samples were then coated by Au/Pd using a gold coater at room temperature and were observed by using secondary electrons via a JEOL 5200 SEM (JEOL-USA Co., Peabody, MA) at an accelerating voltage of 25 kV.

III. RESULTS AND DISCUSSIONS

A. General structure of the sponge spicule

The spicule samples from Rosella are about 0.20–0.6 mm diameter and 10–20 cm long. Each spicule has at its apex a cross-shaped feature with structural characteristics similar to the stem of the spicule. The optically polished cross sections of spicule samples revealed a central core [Fig. 1(d)] and evidence of concentric layers across the diameter [Fig. 1(e)]. The central filament has a square cross section with 7-μm edge length (see also the AFM images of proteinaceous core in Fig. 3). It is known that all sponge spicules have a central proteinaceous filament core with different sizes, cross-sectional shapes, morphologies, molecular compositions, and structure that is mostly crystalline.[16] Although the exact function of this central filament is not clearly known yet, it is speculated that it acts as a nucleation site for the formation of the silica surrounding the core.[17] It is known from previous studies that this core has a highly crystalline structure, and it is present in the spicule in the main stem, as well as in all the side branches, as encountered in some other sponge species. In fact, in Rosella, the central filament extends from the stem to the tip of each arm of the cross-shaped apex [Figs. 1(b) and 1(c)].

B. Nanomechanical properties

Based on the structural data from optical microscopy studies, we conducted nanoindentation measurements of the spicules and compared them with those of glass optical fibers, silica-glass rods, and bulk fused silica samples (Fig. 2). The indentations were made parallel to the spicule axis and at a series of points along the radius, starting at the central core of the spicules and then moving toward the edge. To evaluate whether there was any polar anisotropy, we made indentations in other radial directions [Fig. 3(a)]. In all cases, we consistently obtained hardness values of 3.22 ± 0.33 GPa regardless of the position of the indenter across the diameter of the spicule (except the central filament, see below). In Table I, the standard deviation is a measure of the uniformity of the property value throughout the structure. Similarly, from the *F-d* curves [Fig. 2(a)], we determined the elastic modulus values as $E = 38.05 \pm 2.90$ GPa for the spicules. These mechanical property values of the sponge spicule are about half of those for fused silica or glass rods (see Table I, and also Ref. 18). Glass optical fiber samples were also tested in a similar manner by using the same loading conditions; the hardness and Young's modulus values are 7.80 ± 0.80 GPa and 63.16 ± 3.28 GPa, respectively. These values of *H* and *E* are compared in Table I. The relatively small difference in the properties of fused silica and glass optical fiber are due in part to the fact that optical fiber is not pure silica, but it contains low concentrations of other inorganic components. In addition, optical-grade fibers are solidified glasses with completely disordered structures of silica originally heated to, usually, about 2000 °C.[1,4]

The differences between the nanomechanical properties of the spicule and the optical fiber are more intriguing. Although both the optical glass fiber and the spicule are made of SiO_2, the sponge spicules are known to have intrinsic water in the structure. In other words, the siliceous material in the spicule is $SiO_2 \cdot xH_2O$, i.e., hydrated silica, a biogenic opal! In fact, all spicular or

https://doi.org/10.1557/JMR.2001.0198

skeletal silica are hydrated, and the value x of H_2O changes from 0.25 to 1, depending on the sponge species.[16] Our qualitative comparison between Rosella spicules and Monoraphsis anchoring spicules[19] indicated that the Rosella spicules are more rigid than the anchoring spicules. Monoraphsis spicules are known to contain a large amount of water ($x = 1$).[19] We estimated the value of x being about 0.25 in Rosella spicules. The fact that spicules are composed of hydrated silica would lead to their lower elastic modulus and, hence, softer characteristics than that of the fused silica or glass fiber.

C. Microstructural characterization

We analyzed the microstructure of the spicules in more detail by examining the fractured surfaces of the samples using an SEM. Instead of a fairly smooth fracture surface that would be expected to appear from a solid bar, all the fractured spicules displayed a rough surface with signs of layering. Close examination of such samples revealed that the spicules have a layered structure across the thickness surrounding the central filament. As shown in Figs. 4(a), 4(b), and 4(c), the spicule is composed of concentric cylinders of silica separated with a definite interface. The layered structure of the spicule clearly plays a role in the mechanical properties of the spicule. A relatively weak interface (interlayer) deflects the crack, stopping the crack from propagating directly in to the next layer during fracture[19] (see below Sect. III. D). Presently, detailed characteristics of the interfaces, whether there is any organic material present at the interfaces or there is a structural discontinuity at these locations, are not yet known.

As shown in the optical microscopy and the SEM images, the thickness of the concentric layers varies from 2 to 15 μm, with no apparent uniformity. It was observed, however, that layers close to the central core was somewhat thicker than those near the periphery of the spicules. In fact, in many spicules, but not all, the central filament was surrounded by a 20–40-μm-diameter solid shell of silica [Fig. 4(a)]. The high-magnification image in Fig. 4(b) displays the fractured surface, revealing terraces that were created by the crack deflecting into the interface between the silica layers. In this region, the average thickness of the layers is about 10 μm. We estimated that the total number of the layers to be about 50–200 across the thickness of a given spicule. So far, we have not yet examined the rate of growth of the layers or whether thickness variations of the layers is due to seasonal and nutritional conditions. Furthermore, we have not investigated the mechanism of formation of the layers. Nevertheless, the image in Fig. 4(c) from the fractured surface of a 3-point-bend sample suggests that successive layers throughout the spicule are spirally wrapped around the previous shell inside. If this is proven to be true, then this spiral geometry of the layers allows growth of the spicule, starting from the "root," i.e., at the protruding position on the wall of the sponge. The growth would occur simultaneously both in the longitudinal (along the length) as well as in the transverse (along the thickness) directions. In fact, the thickness of a given layer tapers down toward the very tip of the spicules, i.e., the position just before it is connected to the apex structure. Similarly, the tips of the cross-shaped apex taper down to a conical shape again with spirally wrapped silica layers decreasing in thickness as they reach the tip of each arm of the apex.

D. Bulk mechanical properties

We also tested the spicule samples in 3-point-bending experiments to determine fracture strength and to investigate their failure mechanisms. The strength of the spicules is more relevant in bending rather than in tension, because they are subjected to bending (and possibly torsional) states of stresses in their natural environment. The bulk mechanical properties results were compared with those of silica rods of similar diameter. The most

TABLE I. Mechanical properties of spicule compared rodlike synthetic silica glass materials.

Material	Nanohardness H (GPa)	Elastic modulus[4] E (GPa)	Fracture strength[5] σ_F (MPa)	Fracture toughness[6] (MPa-$m^{1/2}$)	Fracture strain[7] (%)
Optical fiber[1]	7.80 ± 0.80[4]	63.16 ± 3.28[4]	—	—	—
Fused silica	7.50 ± 0.50[4]	70.00 ± 2.00[4]	—	—	—
Silica rod[2]	—	—	200 ± 15[5]	0.78 ± 0.05[8]	1.0 ± 0.1
Sponge spicule[3]	3.22 ± 0.33[4]	38.05 ± 2.90[4]	880 ± 15[5]	2.26–5.60 ± 0.10	3.5 ± 0.1

[1]From Corning Inc.
[2]From General Electric Co.
[3]Rosella.
[4]Nanoindentation.
[5]3-point bend test.
[6]Calculated from Griffith's formula.
[7]From 3-point-bend test.
[8]From Ref. 18.

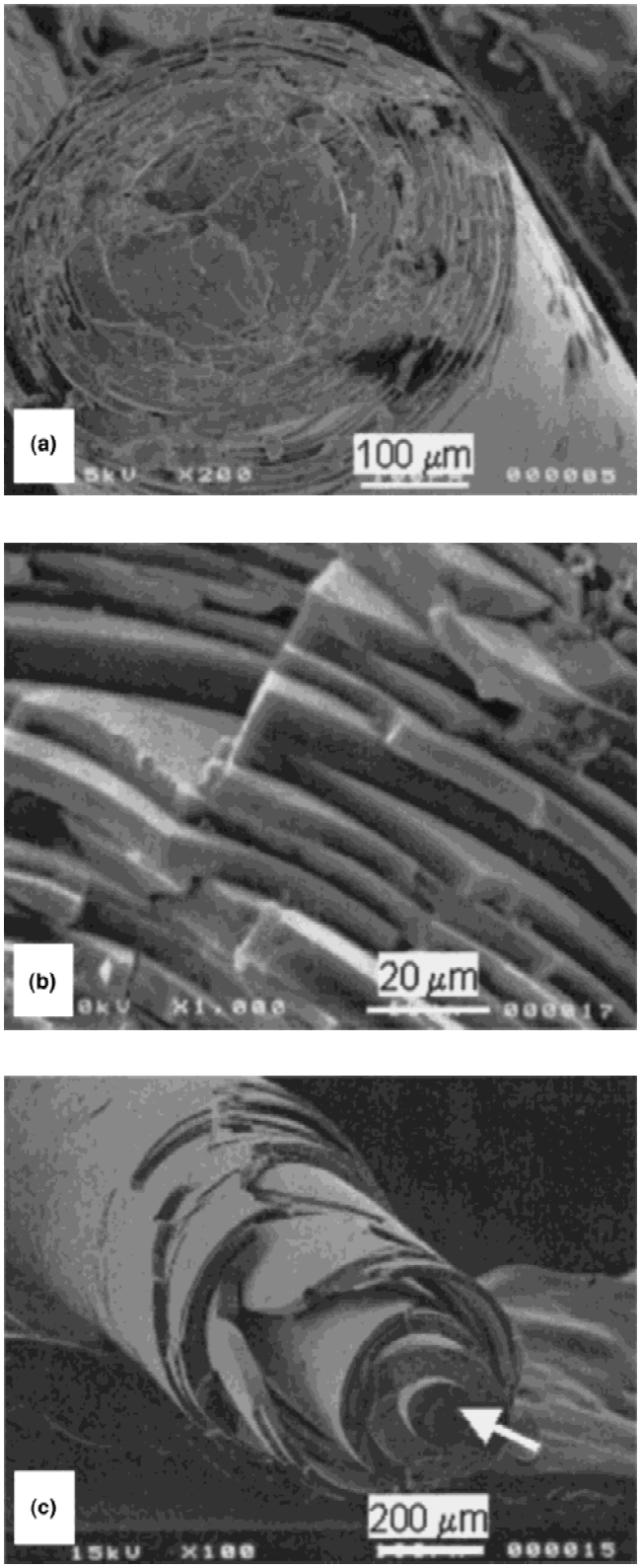

FIG. 4. (a) and (b) are SEM images of the fractured surface of a Rosella spicule showing layering at low and high magnifications, respectively. The sample was fractured after plunging into liquid nitrogen. (c) SEM image of a fractured spicule from a 3-point-bend test. Layering as well as the thick silica shell around the central core is visible.

dramatic results, displayed in Fig. 5, show the stress–strain behavior of sponge spicules and silica rods. The behavior of silica rods is as expected, i.e., as the stress increases, there is only a marginal increase in the elastic strain as in all ceramic glasses. The failure of the silica rod takes place in the elastic regimen because of a catastrophic failure mechanism (sudden drop of stress) at a relatively low strain (<1%) at 200 MPa bending stress. On the other hand, spicules fail at much higher levels of stresses, close to 900 MPa with a substantial, 3–4%, strain! In addition, the stress–strain behavior of the silica spicules reveals a sawtooth behavior during failure. This is an indication of discontinuous crack propagation in a damage tolerant material.[20,21]

An approximate value for the fracture energy[22] can also be calculated by using the area under the stress–strain diagram shown in Fig. 5. As can be seen in this figure, the value of the fracture energy of the spicule is 15–20 times higher than that of the silica rod. It is also tempting to relate the critical crack size that causes fracture of a single silica layer to that of layer thickness (2–10 μm) of the Rosella spicules. Using Griffith's formula[23] [$K_{IC} = \sigma_F Y (\pi c)^{1/2}$], the fracture toughness, K_{IC}, of the spicules can be estimated by using the fracture strength, σ_F, and the layer thickness, 2–10 μm, as the size of the critical crack, c. This approximation gives values for the fracture toughness of the spicules in the range of 2.0–5.0 MPa-$m^{1/2}$. These values are within the range of tough bulk ceramics (such as alumina, silicon carbide, and silicon nitride)[24] and much higher (5–10 times) than that of bulk SiO_2 (whose fracture toughness is 0.79 MPa-$m^{1/2}$).[18] Also using Griffith's criteria and a literature value of 0.78 MPa-$m^{1/2}$ for the fracture toughness of SiO_2 the critical flaw size of the SiO_2 rods was estimated to be 4 μm.

The nature of the discontinuous fracture behavior of the spicule shown in Fig. 5 is explained on the basis of the crack propagation across the diameter of the

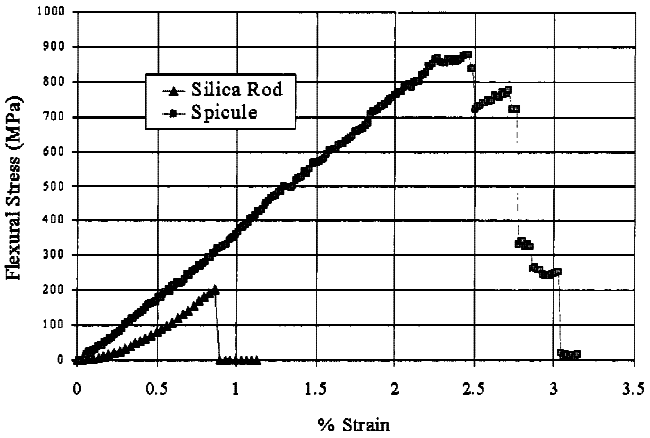

FIG. 5. Stress–strain diagrams of a spicule and a glass rod tested in 3-point-bending.

https://doi.org/10.1557/JMR.2001.0198

spicule. During fracture, the crack does not follow a continuous path through the thickness of the spicule but rather a tortuous path through the layers and along the interfaces between the layers. Once the critical stress is reached, the crack travels through the outermost layer and meanders through the interface before jumping into the next layer at a surface microcrack on that layer. This process, jumping through layers and meandering through interfaces, is repeated many times until the crack travels through all layers across the thickness of the sample. The result of this process is that crack propagation is controlled[25] because of the layered nature of the material and the interface characteristics. The layered microstructure requires considerably more energy to fracture than a solid SiO_2 bar that does not have crack-limiting structures. Also, in the center of the spicule is essentially a tough, proteinaceous filament (see Sec. III. E). This central filament may add to the tenacity of the spicule against catastrophic failure. The combined overall results of the structural features is a significant toughness increase of the spicule.

E. Characteristics of the central proteinaceous filament core

It appears from the SEM [Figs. 1(d) and 1(e)] and the AFM [Figs. 3(a) and 3(c)] images that the central core has a featureless structure, as examined by these techniques. As indicated above, it is believed that this is due to the presence of the proteinaceous material of this filament. The protein filament has a square cross section with an edge length of 7 μm. Nanomechanical tests conducted at the central filament [Fig. 3(c)] indicated that the H and E values are 0.87 ± 0.10 GPa and 11.20 ± 1.00 GPa, respectively. These values are somewhat higher than a typical structural protein.[26] The high values of H and E are possibly due to the fact that the proteins at the core have an ordered structure and display a rigid behavior, i.e., fibrous protein molecules tested in the direction parallel to their long axis. As mentioned above, the proteinaceous core may have a function in the formation of the silica. Some of the major protein components from the central core were isolated in a recent investigation using a Pacific sponge, *Tethya aurantia.*[17] These proteins, called silicateins, have been identified as being enzymes used by the sponge in the catalysis of silica obtained from ions in the seawater.[17] In this case, the spicules (support structures) were exceptionally tiny, with only a 30-μm diameter and about several hundred micrometers long! In Rosella, the protein(s) in the central core, whose characteristics have yet to be determined, may have the same catalysis function. In addition, the fact that this protein core is present in the arms of the cross-shaped apex as well as in the stem may indicate that it also serves as a support structure for the mechanical integrity of the overall architecture of the spicule.

The question still remains whether there are additional macromolecular components (e.g., proteins) present within or between the layers (interlayer and intralayer, respectively). The fact that the hardness and elastic modulus values are half those of fused silica or optical glass fibers may indicate that the intralayer structure may contain occluded proteins in addition to the silica being hydrated, which would both cause a softening of the structure. On the other hand, our nanomechanical properties across the thickness of a given spicule did not show any variation of the properties throughout. This may indicate that, structurally, there is no variation throughout the thickness of the spicule, including the interfaces. However, during nanohardness measurements, interfaces might very easily be missed because they are difficult to reveal in the samples used for nanoindentations. Fractured surfaces as well as the optical microscopy images from etched samples clearly revealed the presence of layering, suggesting that these intralayers are relatively weaker (both mechanically and chemically) than the layered material (i.e., silica). This very fact indicates that there is a discontinuity at the interfaces, and they may very well contain intralayer organic material. This latter point, however, has to be carefully considered and experimentally verified because the existence of any organic interlayer could also have consequences in the formation mechanisms of the spicules themselves.

IV. CONCLUSIONS

We conducted bulk and nanomechanical tests and analyzed microstructure of an Antarctic sponge *Rosella racovitzea* that has known optical characteristics. Some of the conclusions are as follows:

(1) Spicules have a layered structure, with layers parallel to the axis of the spicule.

(2) The tip of the spicules have a cross-shaped apex that retains the layered characteristics.

(3) The layers have a randomly distributed thickness in the range of 2–10 μm through the spicule.

(4) Hardness and elastic modulus values (3.22 ± 0.33 GPa and 38 ± 3 GPa, respectively) of the spicules, determined by using an AFM-based nanomechanical testing are half those of optical grade glass fibers, silica rods, or fused silica.

(5) The central proteinaceous filament has a square cross section 7 μm across and has hardness and elastic modulus 0.87 ± 0.10 GPa and 11.20 ± 1.00 GPa, respectively. These values are considerably higher than those of many known structural proteins.

(6) Stress–strain curves from bulk testing (3-point-bend) of the spicules have a "sawtooth" behavior, indicating stable crack propagation and damage tolerant spicules unlike the behavior of a silica rod, which fails catastrophically.

https://doi.org/10.1557/JMR.2001.0198

(7) Fracture strengths (900 MPa) and fracture toughness (up to 5 MPa-$m^{1/2}$) of the sponge spicules are many times those of a silica rod. Fracture energy is about 15 times of that of a glass silica rod.

ACKNOWLEDGMENT

The authors thank Dr. A. Bleloch (Cambridge University, UK) for discussions during nanoindentations.

REFERENCES

1. L.L. Blyler and F.V. DiMarcello, *Optical Fibers, Drawing, and Coating*, Encyclopedia of Technology Vol. 9 (Academic Press, New York, 1987) pp. 647–657.
2. M.J. Mathewson and D.H.H. Yuce, SPIE **2290,** 204 (1994).
3. R. Cattano-Vietti, G. Bavestrello, C. Cerrano, M. Sara, U. Nenatti, M. Glovine, and G. Giano, Nature **383,** 397 (1996).
4. V.V. Rondinella, M.J. Matthewson, and C.R. Kurkjian, J. Amer. Ceram. Soc. **77,** 73 (1994).
5. S. Mann, Science, **261,** 1286 (1992).
6. M. Sarikaya, Proc. Natl. Acad. Sci. USA **96,** 14183 (1999).
7. T.L. Simpson, *Cell Biology of Sponges* (Springer, New York, 1984).
8. F.E. Schultze, Rep. Scient. Results Challenger Zoology **21** (1887).
9. A. Arillo, G. Bavestrello, G. Burlando, and M. Sara, Mar. Biol. **117,** 159 (1993).
10. E. Giano and M. Sara, Mar. Ecol. Prog. Ser. **108,** 147 (1994).
11. A. Mescher, H. Fong, and M. Sarikaya (unpublished data, 2000).
12. E.G. Rawson and R.G. Murray, IEEE J., Quantum **QE-9,** 1114 (1973).
13. M. Ikada, M. Tadeda, and H. Yoshikiyo, Appl. Optics **14**(4), 814 (1975).
14. M.F. Doerner and W.D. Nix, J. Mater. Res. **1**(4), 601 (1986).
15. W.C. Oliver and G.M. Pharr, J. Mater. Res. **4**(6), 1564 (1992).
16. M.A.R. Koehl, J. Exp. Biol. **98,** 239 (1982).
17. K. Shimizu, J. Cha, G.D. Stucky, and D.E. Morse, Proc. Natl. Acad Sci. USA **95,** 6234 (1998).
18. *Engineering Materials Handbook, Vol. 4: Ceramics and Glasses*, S. Schneider (Vol. Chair) (ASM International, Metals Park, OH, 1991).
19. C. Levi, J.L. Barton, C. Guilemet, E. Le-Bras, and P. Lehuede, J. Mater. Sc. Lett. **8,** 337 (1989).
20. W.J. Clegg, K. Kendall, N.M. Alford, T.W. Button, and J.D. Birchall, Nature **347,** 455 (1990).
21. C.A. Folsom, F.W. Zok, and F.F. Lang, in Proc. Ceramic Eng. and Sci., Vol. 13, No. 78 (American Ceramic Society, Westerville, OH, 1992) pp. 467–474.
22. J. Nakayama, Japan. J. App. Phys. **3,** 422 (1964).
23. A.A. Griffith, Phil. Trans. Roy. Soc. **A221,** 163 (1920).
24. *Fracture Mechanics of Ceramics*, edited by R.C. Bradt and F.F. Lang, Vols. 1 and 2 (Plenum, New York, 1974).
25. M-Y. He and J.H. Hutchinson, Int. J. Solids Str. **25,** 1053 (1989).
26. *Mechanical Design in Organisms*, edited by S.A. Wainwright *et al.* (Princeton Univ. Press, Princeton, NJ, 1976).